Advanced Steel Construction – Vol. 22 No. 4 (2026) 393–406
DOI:10.18057/IJASC.2026.22.4.4

EXPERIMENTAL INVESTIGATION FOR ANTI-SLIPPING PERFORMANCE OF STRUCTURAL CARBON STEEL (Q345B) SLIP-RESISTANT CONNECTIONS WITH PARTICLES EMBEDDED IN CONNECTED PLATES

Jun Zhao [1], Wei-Wei Wu [2], Yang Peng [2] and Jun Dong [2, *]

[1] *School of Civil Engineering and Architecture, Changzhou Institute of Technology, Changzhou 213032, China*
[2] *College of Civil Engineering, Nanjing Tech University, Nanjing, Jiangsu 211816, China*
** (Corresponding author: E-mail: dongjun6488@163.com)*

A B S T R A C T

Friction-type high-strength bolted connections have gradually become popular in steel structure buildings due to their inherent advantages, but their shear resistance capacity still needs to be improved. To better enhance the anti-slip performance of ordinary steel structure connections, this paper proposes an innovative anti-slip connection concept that involves embedding specific particles into the surface of ordinary steel. This method enhances the shear resistance of the connection by increasing the friction coefficient of the contact surfaces, with significant effectiveness. Appropriate particle materials and shapes were selected via theoretical analysis. The concept's effectiveness and feasibility were verified via two static test stages: particle embedding tests on steel plates and anti-slip tests of bolted connections under pre-tension. The study reveals the influence laws of factors such as particle diameter, arrangement pattern, distance from the hole wall, and the magnitude of bolt pre-tension. Results of the particle embedding tests indicate that for 6mm steel plates, when the particle diameter is less than 3.5mm, the embedding load increases approximately proportionally with the number of particles. The anti-slip test indicates that as the diameter and number of embedded particles increase, the connection slip coefficient improves significantly. Embedding 4 particles with a 3mm diameter results in a connection anti-slip coefficient of 2.8. The new particle-embedded connection outperforms friction-type high-strength bolted connections in maintaining stable anti-slip loads, highlighting its potential for engineering applications.

A R T I C L E H I S T O R Y

Received: 2 January 2026
Revised: 5 January 2026
Accepted: 9 January 2026

K E Y W O R D S

Ordinary steel;
Embedded particles;
Anti-slip coefficient;
Anti-slip performance

1. Introduction

Steel structure connections are the key to ensuring structural safety and stability [1-3], and the slip resistance of bolted connections directly determines their bearing capacity [4-7]. For high-rise buildings, heavy industrial structures and other key projects, the requirement for the slip resistance coefficient of connections is usually ≥ 1.0 [8-10], but the existing methods are difficult to meet this demand, so it is urgent to develop a new high-efficiency slip resistance improvement technology [11-13].

Existing methods to improve the slip resistance of bolted connections mainly focus on surface treatment (grinding, sandblasting, painting, etc.) and bolt type optimization [14-16]. Scholars have conducted relevant research on this [17-19]. Common methods in construction are as follows: Grinding with a grinding wheel, sandblasting or shot peening, applying inorganic zinc-rich paint after sandblasting or shot peening, generating red rust after sandblasting or shot peening. (1) Grinding with a grinding wheel [20]. The effect after treatment is difficult to stabilize, and the operation process is cumbersome. (2) Sandblasting or shot peening [21]. Under conventional treatment conditions, shot peening has a better effect than sandblasting, and shot peening can be reused. (3) Applying inorganic zinc-rich paint after sandblasting or shot peening [22]. If the steel is exposed to the air without treatment after sandblasting or shot peening, it is prone to secondary rusting. To avoid this situation, inorganic zinc-rich paint is often applied in the later stage of construction [23]. During spraying, tape is pasted near the screw holes to avoid spraying on unnecessary places. (4) Generating red rust after sandblasting or shot peening [24]. After sandblasting or shot peening the surface of the steel plate, no relevant treatment is done on the plate surface, and a layer of red rust formed on its surface is used to increase the roughness of the steel plate. After red rust is formed on the surface of the steel plate, the loose rust is removed without damaging the red rust surface. Because the rust surface method is difficult to control the rusting time and rusting degree, it is rarely used in large steel structural parts. However, these methods for increasing the friction coefficient of contact surfaces in components have notable limitations and limited effectiveness. With the increase in the height of modern buildings and the complexity of functions, bolt connections have also kept up with the development: simplified construction, use of new materials, development of new products, etc [25].

This paper proposes a new type of high-efficiency steel structure anti-slip connection method of particle-embedded anti-slip connection to increase the friction coefficient of the contact surfaces of components. Through two stages of static tests, the test of embedding particles into the steel plate and the connection anti-slip test after applying pre-tension to the bolts, the influence laws of factors such as particle diameter, arrangement mode, distance from the hole wall, and the magnitude of bolt pre-tension are revealed.

2. Selection of test materials

2.1. Selection of connecting steel plates and bolts

The specimen material adopts Q345B ordinary steel plates with dimensions of 300mm × 40mm × 6mm. The bolts used are 8.8-grade high-strength external hexagon bolts with a nominal diameter of 6mm and a length of 25mm. In order to provide a theoretical reference for the load required for subsequent particle embedding into the steel plate and the load of the steel plate before the particles push to form plows, a material property test of the steel plate should be carried out first to obtain the yield strength f_y and tensile strength f_u of the steel plate. The measured dimensions of the specimens and the test results are listed in Table 1. It can be concluded that the yield strength of the connecting steel plate is 457.06 MPa, and the tensile strength is 539.51 MPa.

Table 1
Mechanical properties of ordinary steel plates

Specimen	Thickness t(mm)	Width b(mm)	Cross-sectional area A (mm²)	Tensile strength f_u (Mpa)	Average value of f_u (MPa)	Yield strength f_y (MPa)	Average value of f_y (MPa)
C6-1	5.7	15.00	85.50	546.20	539.51	466.48	457.06
C6-2	5.7	15.00	85.50	542.37		462.59	
C6-3	5.7	15.00	85.50	537.55		452.58	
C6-4	5.8	15.00	87.00	531.93		446.57	

Note: For all specimens, dimensions were measured at 3 positions in the test section, and the minimum cross-sectional dimension in the table is the smallest of the measured values.

2.2. Selection of embedded-in particles

A suitable particle shape can effectively reduce the difficulty of embedding particles into the connecting plate, facilitating manual operation. GCr15 bearing steel balls have higher hardness, so they are selected as the particles to be embedded in. The particle diameters are 1.5mm, 2mm, 2.5mm, 3mm, and 3.5mm respectively.

3. Particle embedding test

3.1. Design of particle embedding test

This test is a room-temperature compression test, conducted on a CSS-44100 electronic universal testing machine. Particles were fixed at specific positions on the steel plate surface using double-sided tape to ensure centering, as illustrated in Fig.1. The loading system is controlled by displacement, with a loading speed of 2mm/min, until the upper and lower steel plates are in complete contact and compressed without any gaps. The criterion for judging the tight contact of the plates is that no light can pass through them, as shown in Fig.2.

3.2. Phenomena and data of embedding tests

3.2.1. Embedding particles with a diameter of 2mm or less into connecting steel plates

In the test, GCr15 bearing steel particles with the same diameter but different quantities were embedded into the connecting steel plates as required, and the arrangement of the particles is shown in Fig.3. After the test, the failure morphology of the particles and the surface of the connecting plate was observed, as shown in Fig.4. The particles can be easily taken out after the test, and they are smooth without deformation. The dents on the surface of the connecting plate are clear, and there are no cracks or bulges around them, indicating that the test effect is very good. For the groups with two or more particles, the distance between particles, which is 5 times the particle diameter, was taken as the variable control factor.

Fig. 1 Fix the particle position

Fig. 2 Fully embedded into the steel plate

Fig. 3 Particle layout

Fig. 4 Test effect diagram of embedding into 1.5mm particles

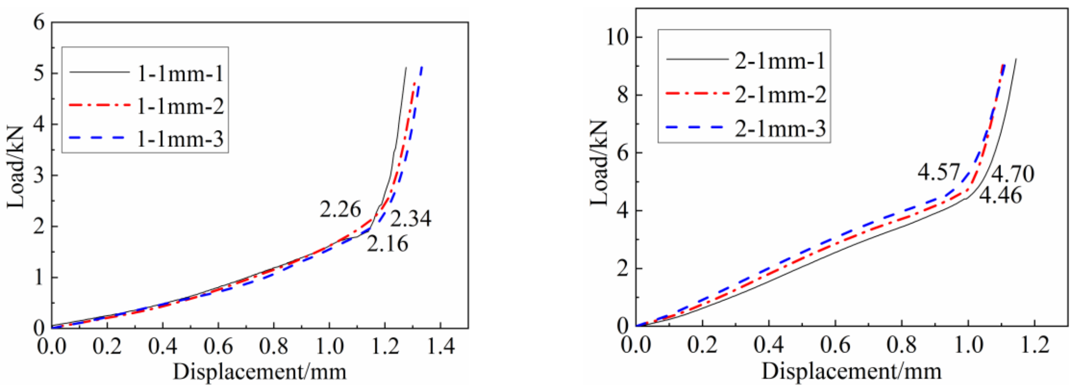

(a) 1-1mm (b) 2-1mm

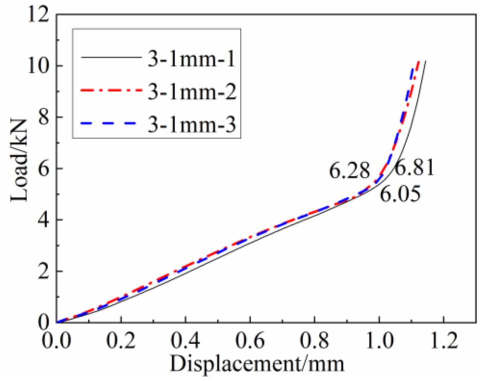

(c) 3-1mm

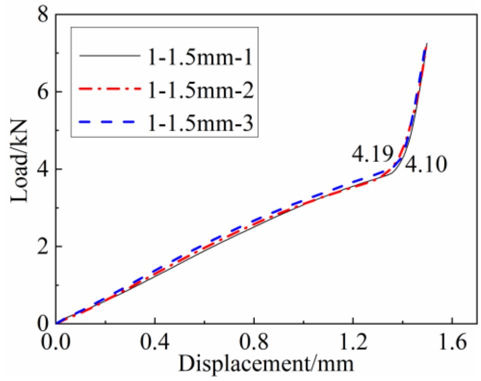

(d) 1-1.5mm

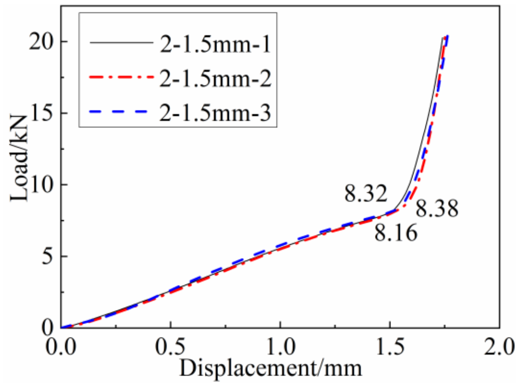

(e) 2-1.5mm

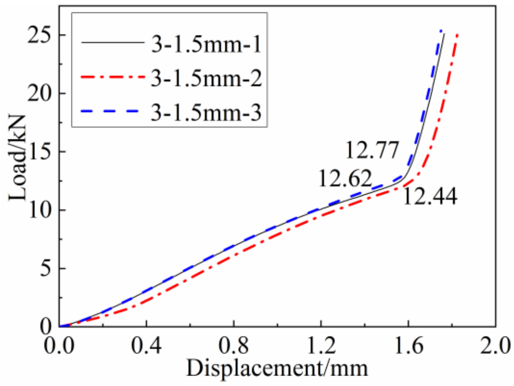

(f) 3-1.5mm

Fig. 5 Load-displacement curves of embedding different numbers of particles

Table 2
Average minimum embedded load

Particle diameter	Load (kN)	1 particle	2 particles	3 particles
1 mm	1	2.16	4.46	6.80
	2	2.26	4.57	6.28
	3	2.34	4.70	6.04
	Average	2.25	4.58	6.37
1.5mm	1	4.10	8.16	12.44
	2	4.10	8.32	12.62
	3	4.19	8.38	12.77
	Average	4.13	8.29	12.61

(1) Test data of embedding 1mm and 1.5mm particles into connecting steel plates

It can be seen from Fig.5 that the process of embedding particles into the connecting plate is smooth and stable, and the curves have a high degree of coincidence. This reflects that the particle embedding process and its minimum embedding load can be stably controlled in actual operation, ensuring that the particles are completely embedded in. The specific data are shown in Table 2. The minimum load required to embed particles into the steel plate basically increases in multiples as the number of particles increases, which also proves the reliability of the experimental data to a certain extent.

(2) Embedding 2mm particles into the connecting steel plate

In accordance with the test requirements, 2mm-diameter particles were embedded into the connecting plate in different quantities, and the arrangement of the particles is similar to that shown in Fig.6. After the test, the failure morphology of the particles and the surface of the connecting plate was observed. The particles could be easily taken out after the test, with a smooth surface and no deformation. The dents on the surface of the connecting plate were clear, and there were no cracks or bulges around them, indicating that the test effect was good. The load-displacement curves and specific data for different numbers of particles are shown in Fig.7.

Fig. 6 Test effect diagram of embedding into 2mm particles

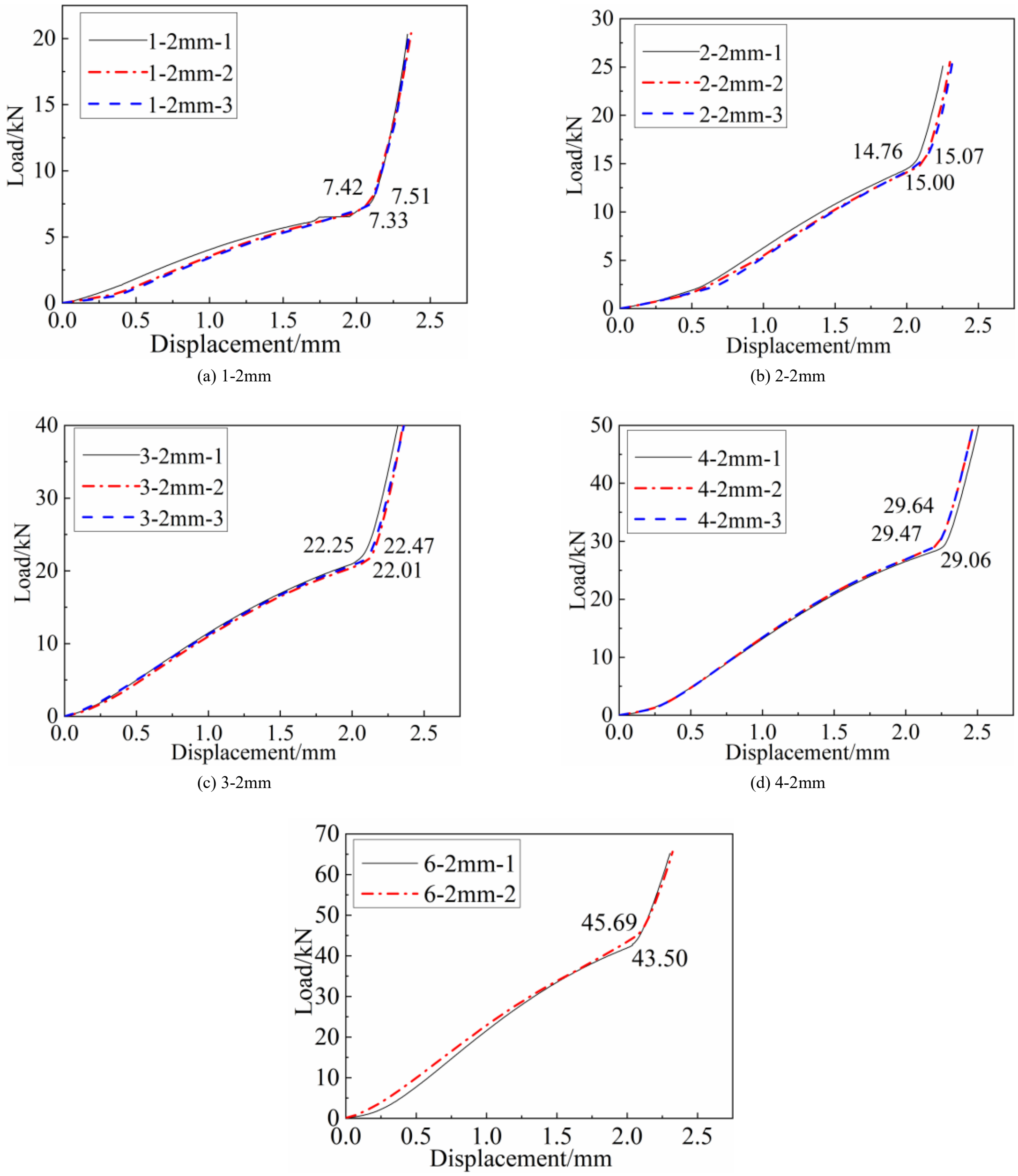

(a) 1-2mm (b) 2-2mm (c) 3-2mm (d) 4-2mm (e) 6-2mm

Fig. 7 Load-displacement curves of embedding different numbers of particles

The process of embedding particles into the connecting plate is smooth and stable, with a high degree of curve coincidence. This indicates that the particle embedding process and its minimum embedding load can be stably controlled, ensuring that the particles are completely embedded in. The specific data are shown in Table 3.

Table 3
Average minimum embedded loads

Particle diameter	Load (kN)	1 particle	2 particles	3 particles	4 particles	6 particles
2mm	1	7.41	14.76	22.47	29.06	43.50
	2	7.33	15.00	22.01	29.47	45.69
	3	7.50	15.07	22.25	32.32	45.69
	Average	7.41	14.94	22.24	30.28	44.96

The minimum load required to embed particles into the steel plate basically increases in multiples as the number of particles increases, and 2mm diameter particles are suitable for this connection.

3.2.2. Embedding large-diameter particles into connecting steel plates

Due to the relatively large particle size of 3.5mm particles, in order to detect whether the particles are deformed or crushed during the embedding process, the same particle was repeatedly embedded in the test. It was found that the particles were almost undamaged, and no deformation was observed when measured with an electronic digital caliper. There was no damage to the particles caused by the embedding of the stainless steel connecting plate, which indicates that particles of this size can maintain their shape well during the connection anti-slip test and fully exert their shear resistance in the connection. The embedded holes were observed under magnification, showing smooth edges without roughness, and a slight sense of protrusion was felt when touching around the furrows by hand, as shown in Fig.8. It can be seen that the 3.5mm diameter particles match the steel plate well. The load-displacement curves and specific data for different numbers of particles with diameters of 2.5mm, 3mm, and 3.5mm are shown in Fig.9 and Table 4.

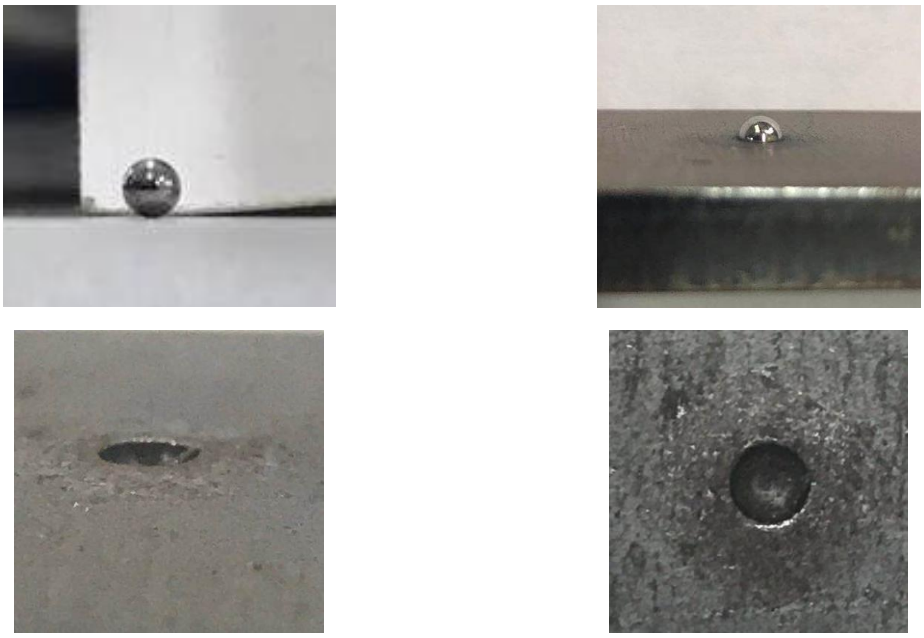

Fig. 8 Test effect diagram of embedding into 3.5mm particles

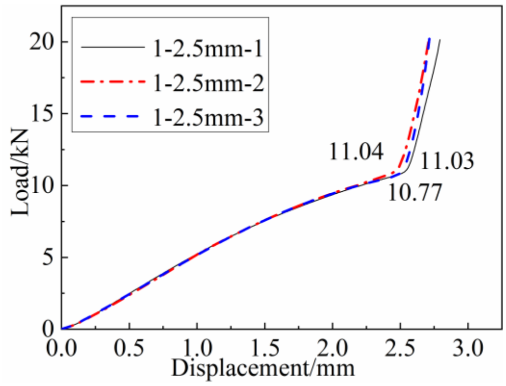

(a) 1-2.5mm

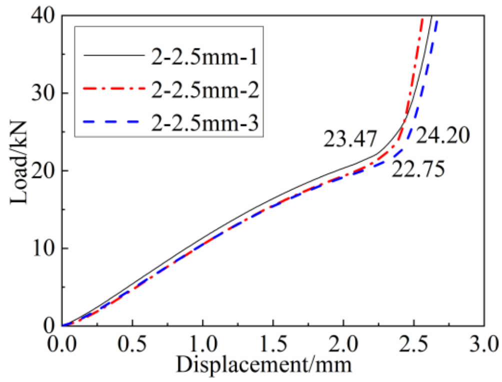

(b) 2-2.5mm

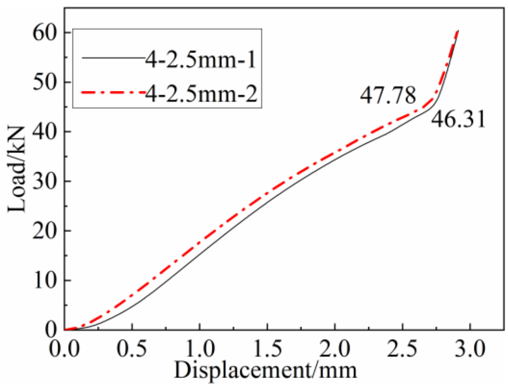

(c) 4-2.5mm

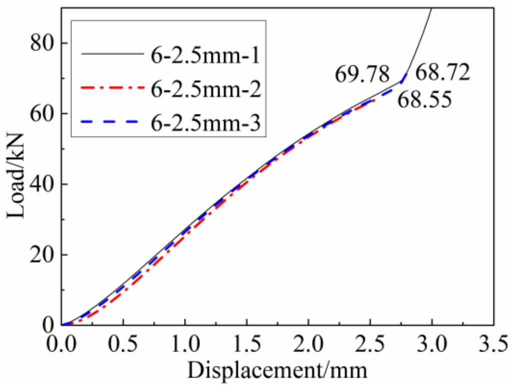

(d) 6-2.5mm

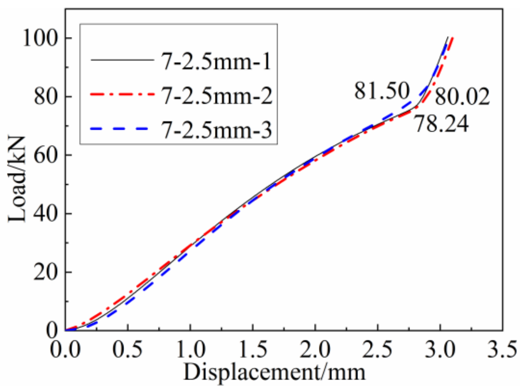

(e) 7-2.5mm

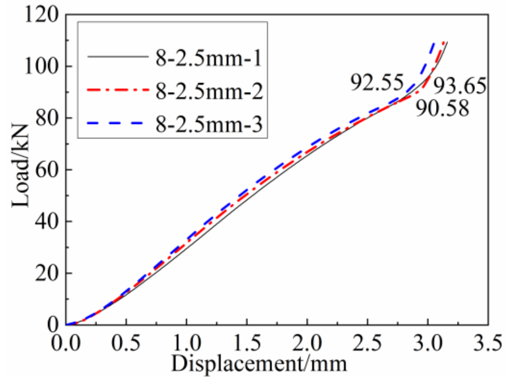

(f) 8-2.5mm

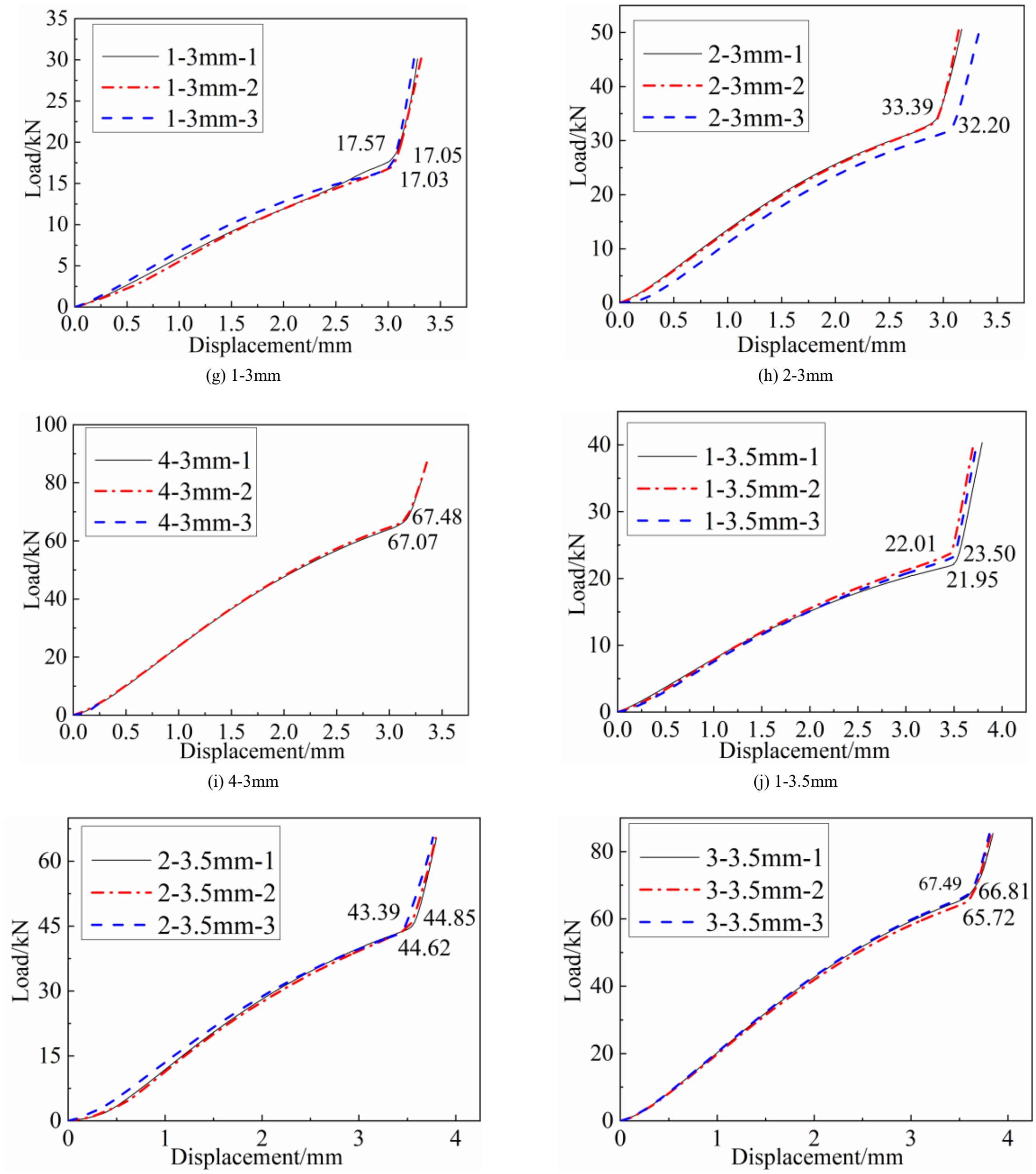

(g) 1-3mm (h) 2-3mm

(i) 4-3mm (j) 1-3.5mm

(e) 2-3.5mm (e) 3-3.5mm

Fig. 9 Load-displacement curves of embedding different numbers of particles

Table 4
Average minimum embedded loads

Particle diameter	Load (kN)	1 particle	2 particles	3 particles	4 particles	6 particles	7 particles	8 particles
2.5mm	1.00	10.77	22.75		46.31	68.55	78.24	90.58
	2.00	11.03	23.47		47.78	68.72	80.02	92.55
	3.00	11.04	24.20		47.78	69.78	81.50	93.65
	Average	10.95	23.47		47.29	69.02	79.92	92.26
3mm	1	17.03	33.39		66.92			
	2	17.05	33.39		66.92			
	3	17.57	32.20		66.92			
	Average	17.22	32.99		66.92			
3.5mm	1	21.95	43.39	65.72				
	2	22.01	44.62	66.81				
	3	23.50	44.85	67.49				
	Average	22.49	44.29	66.67				

Like small-diameter particles, the minimum load required to embed particles into the steel plate basically increases in multiples as the number of particles increases, which indicates that within a certain range of particle diameters, the number of particles does not affect the embedding load value of a single particle.

3.3. Theoretical analysis of particle embedding test

Furthermore, to clarify the relationship between particle size and embedded load, the data obtained from the experiment were sorted out, and it was found that with the increase of particle diameter, the increase of the minimum indentation load value was not proportional to the increase of particle volume, as shown in Table 5.

Table 5
The relationship between the embedded loads and the volume of the particles

Particle diameter/mm	Particle volume/mm^3	Volume increase multiple	Embedded load/kN	Load increase multiple
1	0.52		2.25	
1.5	1.77	3.38	4.20	1.87
2	4.19	8.00	7.41	3.29
2.5	8.18	15.63	10.95	4.87
3	14.14	27.00	17.22	7.65
3.5	22.45	42.88	22.49	10.00

Considering the need to gain an in-depth understanding of the extent to which particle size affects the indentation load and to provide reference specifications for the future engineering application of this new type of connection, this paper has fitted relevant calculation equations based on experimental data, the square of the fitting correlation coefficient is 0.9976, which indicates that the fitting degree of the curve is very good. Thus, Eq.(1) can be obtained.

$$F_e = \beta(2.06d^2 - 1.0529d + 1.1914) \quad (1)$$

Where: β -Correction coefficient (greater than 1); d -Particle diameter; F_e -Minimum indentation load of the particle. The correction coefficient β (β > 1) reflects the hardness matching relationship between particles and steel plates, and is associated with the Brinell hardness formula. Combined with experimental data, the value range of β is 1.2~1.5, which is positively correlated with the Brinell hardness of Q345B steel (HB=190~235) and GCr15 steel (HB=600~700). β can be pre-estimated through the material hardness value.

4. Anti-slip performance test

4.1. Test design

Q345B steel plates are used as connecting plates, with dimensions of 300mm × 40mm and a thickness of 6mm; the particles embedded into the steel plates are GCr15 bearing steel particles, with particle diameters of 1.5mm, 2mm, 2.5mm, and 3mm respectively; the bolts used for connection are 8.8-grade high-strength outer hexagon bolts with a diameter of 6mm. In order to effectively determine the anti-slip performance of the embedded particles, this test adopts a typical single-friction-surface and single-bolt pre-tightened bolt connection form, as shown in Fig.10. However, it should be emphasized that the single-shear test has limitations: when multiple particles are arranged, the warpage of the plate end leads to poor fit between particles and indentations.

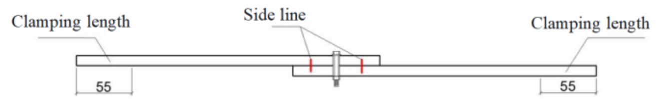

Fig. 10 High-strength bolt connection methods

The anti-slip effect of embedded particles was tested under the conditions of different numbers of particles and different particle diameters. Since the number of particles arranged is not large, double-sided tape marked with position points was not customized. In the experiment, specific diameter circles were drawn on white paper in advance and specific points were marked, then the circles were cut out and placed at the designated positions on the connecting plate, so that specific points could be marked on the connecting plate, as shown in Fig.11. This process is simple and easy to operate, with high accuracy, and the marking paper can be reused.

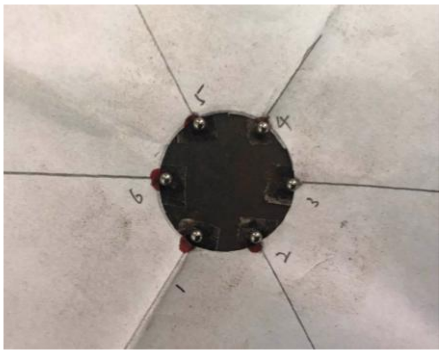

Fig. 11 Actual operation diagram of particle layout

After keeping the test piece embedded tightly, connect it with high-strength bolts and tighten them. Since there is only one bolt, a torque wrench is used to directly tighten it to the final torque value, and it is ensured that the steel plate does not shift during the tightening process. This test is an indoor normal-temperature tensile test, which is carried out on the WAW-600-G microcomputer-controlled electro-hydraulic servo universal testing machine. Both ends of the test piece are fixed and clamped, as shown in Fig.12. The test loading system was displacement-controlled in accordance with specifications, with a loading rate of 2 mm/min. The tensile process continues until the bolt shank is sheared off, which is observed on the load-displacement curve as a sharp drop in bearing capacity.

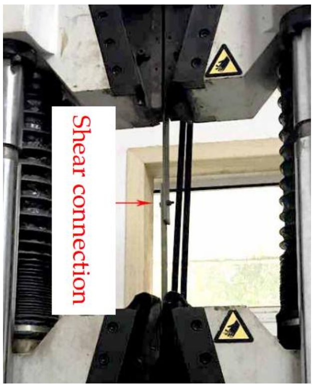

Fig. 12 Equipment for the anti-slip tests

Through 10 sets of experiments tested with a torque wrench, it is found that the breaking torque is all around 27 N·m, so T_t is set as 27 N·m. The average ultimate bearing capacity when the bolt is pulled off is 23.45 kN. Calculated by the equation $k = T_t / dP_t$, we can get $k = 0.19$. To ensure that the steel plate firmly clamps the particles so that their shear resistance can be fully exerted: Take $T = 9.78 N\cdot m$, $T = 90\% T_t = 24.3 N\cdot m$ for comparison; When $T = 24.3 N\cdot m$, $P = T / kd = 21.32 N\cdot m$; When $T = 9.78 N\cdot m$, $P = T / kd = 8.58 N\cdot m$.

To clarify the performance of the connection under repeated loads, cyclic load tests and vibration tests were carried out. The 10,000 cyclic load tests (load amplitude is 50% of the ultimate load) show that the particles have no looseness, the indentation deformation is ≤ 0.02mm, and the pre-tension loss is ≤ 5%, which is much lower than the pre-tension loss of friction-type high-strength bolts (about 15%). Vibration tests (frequency 10~100Hz, acceleration 0.5g) show that the attenuation of the slip resistance coefficient of the connection is ≤ 8%, which meets the long-term use requirements of industrial structures.

4.2. Phenomena and data of anti-slip tests

4.2.1. Anti-slip test of connections under a bolt pre-tension of 8.58kN

The test was stopped when the computer showed a sharp drop in the anti-slip bearing capacity of the connection. At this point, the connection had suffered shear failure. It was observed that the steel plates had obvious misalignment, and the plate ends were warped, though not significantly, as shown in Fig.13. When the connection was disassembled, plow furrows caused by the misalignment of the plates and the extrusion of the particles could be seen on the surfaces of the two connecting steel plates. The surfaces of the plow furrows were smooth, with no cracks or visible deformation around them, and there were protrusions at the ends of the plow furrows caused by the pushing of the particles. All the particles were located on one of the connecting steel plates, and no fragmentation or damage was observed after they were taken out, as shown in Fig.14.

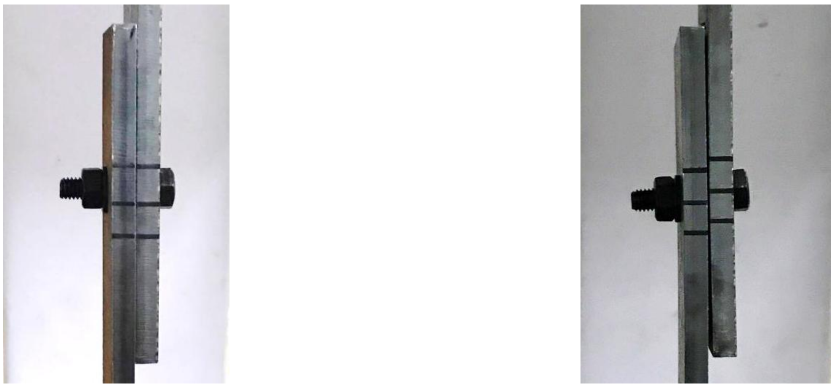

Fig. 13 Failure of bolt connection after testing

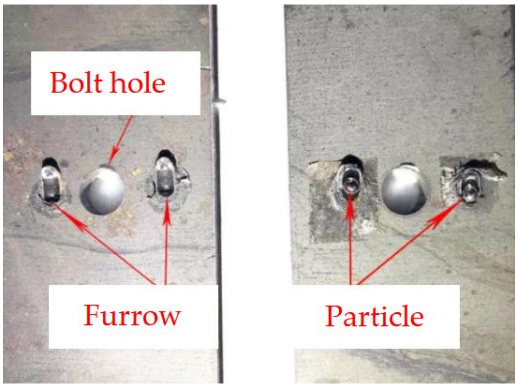

Fig. 14 Furrow on the plate and embedded particle

The load-displacement curves of the anti-slip tests for connections with particles of different quantities embedded into the steel plate surface to a depth of 2mm are shown in Fig.15. The specific test data are shown in Table 6. Embedding particles into the surface of Q345B steel structures can significantly improve the anti-slip coefficient of the connections. After embedding 1, 2, and 4 particles of 2mm into the connecting plate, the anti-slip coefficients increased by 97.5%, 155%, and 270% respectively. With the increase in the number of particles, the ultimate slip load also increased.

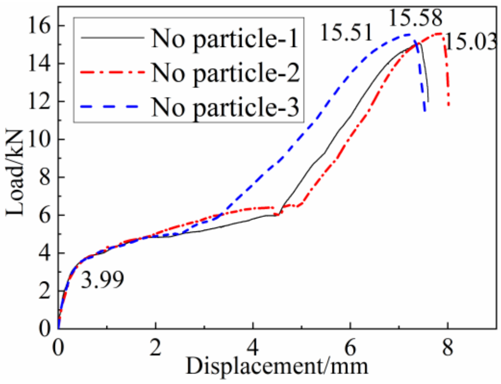

(a) No particle

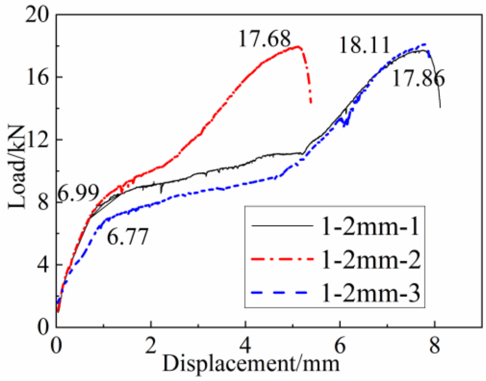

(b) 1-2mm

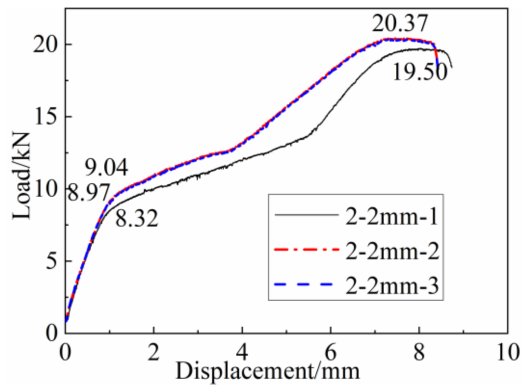

(c) 2-2mm

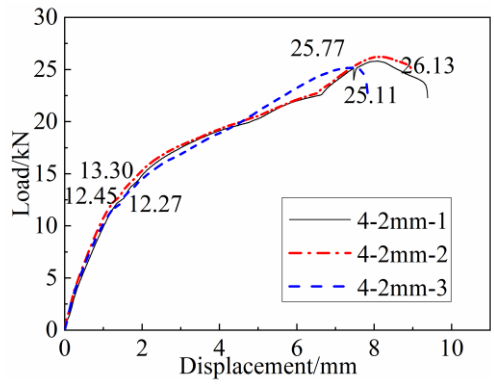

(d) 4-2mm

Fig. 15 Load-displacement curves of anti-slip connections with different numbers of particles

Table 6
Test data on anti-slip connections with different numbers of embedded-in particles

2mm particle		No particle	1 particle	2 particles	4 particles
Critical load F_{sc} /kN	1	3.39	6.99	8.32	13.30
	2	3.39	6.99	9.04	12.45
	3	3.39	6.32	8.97	12.27
	Average	3.39	6.77	8.78	12.67
	Anti-slip coefficient μ	0.40	0.79	1.02	1.48
Ultimate load F_{su} /kN	1	15.03	17.68	19.50	25.77
	2	15.51	17.86	20.37	26.13
	3	15.58	18.11	20.37	25.11
	Average	15.37	17.88	20.08	25.67

The load-displacement curves of the anti-slip tests for connections with particles of different quantities embedded into the steel plate surface to a depth of 2.5mm are shown in Fig.16. The specific data are shown in Table 7. After embedding 1, 2, 4, and 6 particles with a diameter of 2mm, the anti-slip coefficients increased by 170%, 260%, 405%, and 535% respectively. A comparison of the data shows that the "anti-slip efficiency" of the connection after embedding particles with a diameter of 2.5mm into the steel plate is equivalent to twice the effect achieved by embedding particles with a diameter of 2mm. Moreover, the connection has the advantages of simple operation, stable force bearing, and remarkable effect during the processing and the process of bearing slip load. To explore the limit of particle size under this scenario, the test continued to try increasing the particle size.

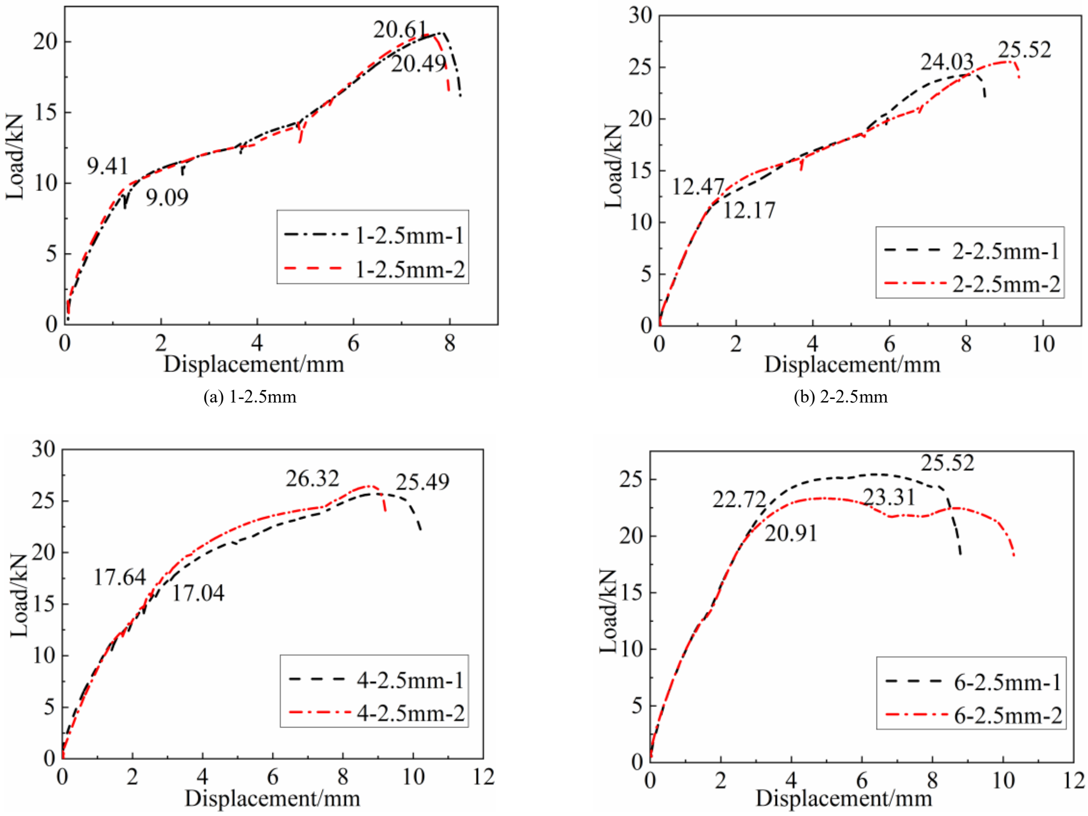

(a) 1-2.5mm (b) 2-2.5mm

(c) 4-2.5mm (d) 6-2.5mm

Fig. 16 Load-displacement curves of anti-slip connections with different numbers of particles

Table 7
Test data on anti-slip connections with different numbers of embedded-in particles

2.5mm particle		1 particle	2 particles	4 particles	6 particles
Critical load F_{sc} /kN	1	9.09	12.17	17.04	20.91
	2	9.41	12.47	17.64	22.72
	Average	9.25	12.32	17.34	21.82
	Anti-slip coefficient μ	1.08	1.44	2.02	2.54
Ultimate load F_{su} /kN	1	20.61	24.03	25.49	23.31
	2	20.49	25.52	26.32	25.41
	Average	20.55	24.78	25.91	24.36

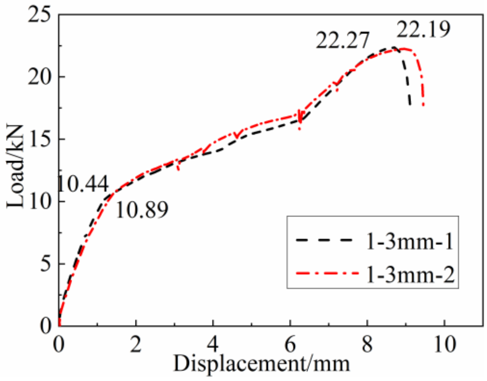

(a) 1-3mm

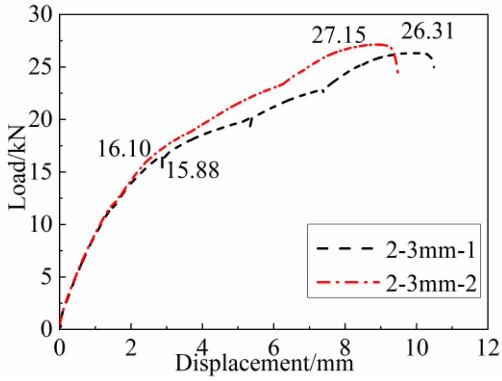

(b) 2-3mm

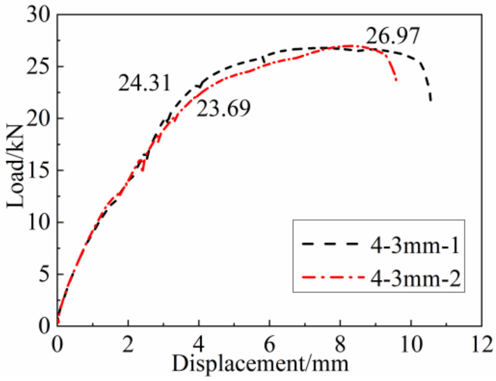

(c) 4-3mm

Fig. 17 Load-displacement curves of anti-slip connections with different numbers of particles

Table 8
Test data on anti-slip connections with different numbers of embedded-in particles

3mm particle		1 particle	2 particles	4 particles
Critical load F_{sc} /kN	1	10.44	15.88	23.69
	2	10.89	16.10	24.31
	Average	10.67	15.99	24.00
	Anti-slip coefficient μ	1.24	1.86	2.80
Ultimate load F_{su} /kN	1	22.27	26.31	26.79
	2	22.19	27.15	26.79
	Average	22.23	26.73	26.79

The load-displacement curves of the anti-slip tests for connections with particles of different quantities embedded into the steel plate surface to a depth of 3mm are shown in Fig.17. The specific data are shown in Table 8. After embedding 1, 2, and 4 particles with a diameter of 3mm, the anti-slip coefficients increased by 210%, 365%, and 600% respectively. The anti-slip effect of particles with a diameter of 3mm has been significantly improved compared with that of particles with a diameter of 2.5mm. After embedding 4 particles into the steel plate, the anti-slip coefficient of the connection reached 2.80, which is much higher than the effect obtained by conventional treatment methods on the surface of the connecting plate.

Compared with small-diameter particles, the plow furrows left on the surface of the steel plate after the failure of the connection with 3mm-diameter steel balls are more obvious, and the accumulations formed by pushing the surface of the steel plate are also higher. Due to the limitation of the selected thickness of the connecting plate, it is not advisable to continue increasing the size of the particles to avoid invisible internal damage to the connecting plate, as shown in Fig.18. Under repeated loads, the connection has good stability: the particles do not loosen, the indentation deformation is small, and the pre-tension loss is low, which can meet the long-term service requirements of industrial structures. The minimum ratio of plate thickness to particle diameter (t/d) is recommended to be ≥ 1.7. At this ratio, the connecting plate has no internal damage and the anti-slip performance is stable.

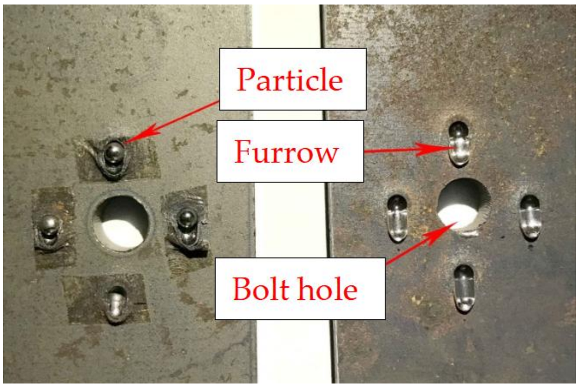

Fig. 18 Furrow on the plate and embedded particle

4.2.2. Anti-slip test of connections under a bolt pre-tension of 21.32kN

Considering the influence of different pretension forces on the new type of connection, the test added a pretension force of P = 21.32 kN as the control group. The load-displacement curves of the anti-slip tests for connections with particles of different quantities embedded into the surface to a depth of 2mm are shown in Fig.19. The specific data are shown in Table 9.

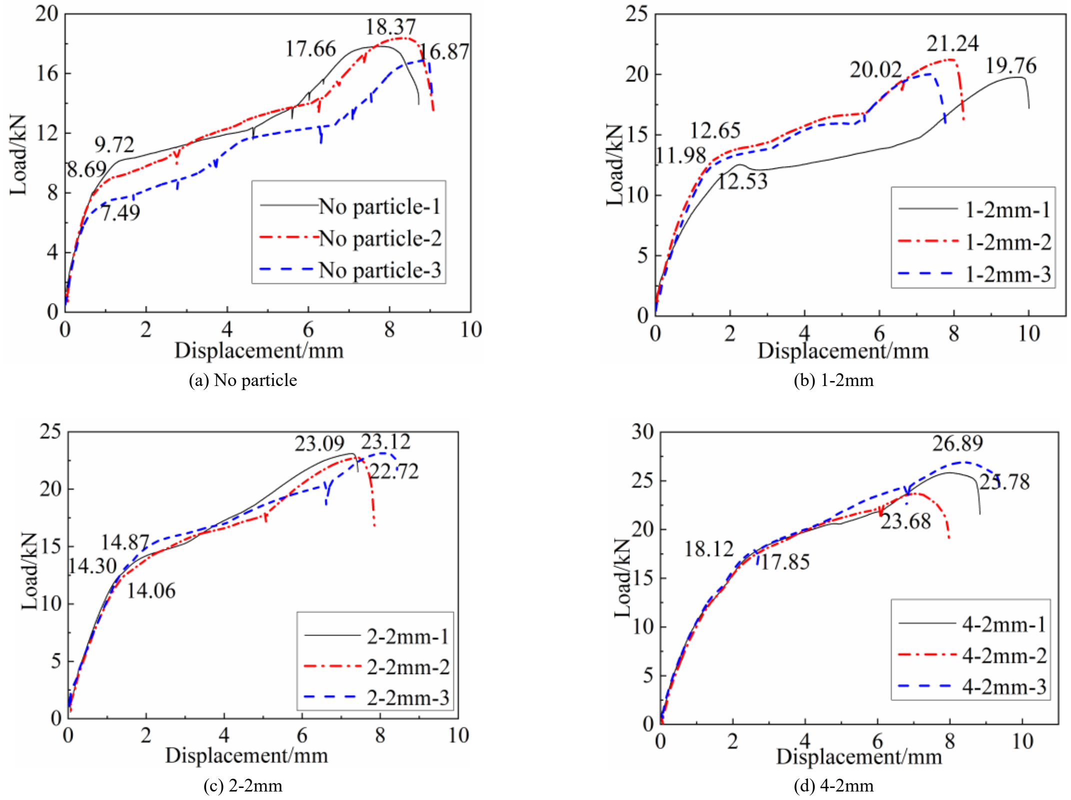

(a) No particle (b) 1-2mm

(c) 2-2mm (d) 4-2mm

Fig. 19 Load-displacement curves of anti-slip connections with different numbers of particles

Table 9
Test data on anti-slip performance of connections with different numbers of embedded-in particles

2mm particle		No particle	1 particle	2 particles	4 particles
Critical load F_{sc} /kN	1	9.72	12.53	14.30	17.85
	2	8.69	12.65	14.06	17.85
	3	7.49	11.98	14.73	18.12
	Average	8.63	12.39	14.36	17.79
	Anti-slip coefficient μ	0.40	0.58	0.67	0.84
Ultimate load F_{su} /kN	1	17.66	19.76	23.09	25.78
	2	18.37	21.24	22.72	23.68
	3	16.87	20.02	23.12	26.89
	Average	17.63	20.34	22.98	25.45

A comparison of Tables 6 and 9 shows that with the increase of pretightening force, the anti-slip coefficient of the connection without embedded particles remains unchanged, which is in line with the law of friction, and both the critical load and ultimate load increase. After embedding 1, 2, and 4 particles of 2mm into the connecting plate, the anti-slip coefficients increased by 45%, 67.5%, and 110% respectively.

4.3. Analysis of connection anti-slip test

4.3.1. Influence of particle diameter on anti-slip load of the new connection

A vertical comparison of the data in Table 10 reveals that when the pretension force of the connection is fixed, the anti-slip load of the connection increases significantly as the particle diameter increases.

Table 10
The anti-slip load of the new type of connection

Pretension /kN	Particle diameter d/mm	1 particle	2 particles	4 particles	6 particles
	2	6.77	8.78	12.67	
8.58	2.5	9.25	12.32	17.34	21.82
	3	10.67	15.99	24	

To process the critical load data more clearly, this research divides the load into the sum of the friction force N_f between the connecting plate surfaces and the anti-slip load N_{pv} provided by the particles, which is expressed by Eq.(2):

$$F_{sc} = N_f + N_{pv} \tag{2}$$

Where, F_{sc} -Critical anti-slip load; N_f -Friction force between the connecting plate surfaces (the anti-slip load of the connection when no particles are embedded in); N_{pv} -Anti-slip load provided by the particles;

Since this paper mainly studies the anti-slip load N_{pv} provided by particles, the critical anti-slip load F_{sc} data in Table 10 is subtracted by the friction force N_f between the connecting plate surfaces to obtain Table 11.

Table 11
The anti-slip load of the new type of connection

Pretension/kN	Particle diameter d/mm	1 particle	2 particles	4 particles	6 particles
	2	3.38	5.39	9.28	
8.58	2.5	5.86	8.93	13.95	18.43
	3	7.28	12.60	20.61	

The slip resistance of the particle-embedded connection is similar to that of the woodruff key, where the particles play a role of "locking" to prevent relative slip between the connecting plates. However, the woodruff key analogy has limitations, so the "three-dimensional constrained particle shear model" is proposed to clarify the slip resistance mechanism: the slip resistance of particles comes from the shear deformation and the plastic flow resistance of the material around the indentation, Eq.(3) is derived:

$$f_{pv} = \frac{8N_{pv1}}{\pi d^2} \tag{3}$$

Where, N_{pv1} -Anti-slip load provided by a single particle (N); d -Particle diameter (mm); f_{pv} -Strength of the contact area of the indentation on the surface of the connecting plate (MPa).

The strength of the contact area of the indentation on the connecting plate surface was calculated for single particles with different diameters, based on Eq.(3), as shown in Table 12.

Table 12
Contact area strength of indentations on the surface of connecting plates

Particle diameter d/mm	2	2.5	3
Strength f_{pv} / MPa	2149.65	2387.58	2058.41

To further understand the strength of the contact area of the indentation on the surface of the connecting plate, reference is made to the concept of the bearing strength of hole walls involved in the bearing connection of high-strength bolts. In Chapter 2, a tensile test on the mechanical properties of the connecting steel plate was conducted, the lower yield strength of the connecting steel plate is 457.06 MPa, and the minimum tensile strength is 539.51 MPa. The bearing strength of the steel plate is only related to the tensile strength of the steel plate, and has no direct connection with the yield strength of the steel plate. According to the provisions in GB50017-2017 [26], the hole wall bearing strength of several steels from Q235 to Q460 can be calculated by Eq.(4).

$$f_c = 1.26 f_u \tag{4}$$

The obtained hole wall bearing strength is 679.78 MPa, which is much lower than the data in Table 12. The strength of the connecting plate in the contact area of the particle indentation, under the environment of triaxial compression, is much higher than its bearing strength, which fully ensures the anti-slip performance of the particles.

4.3.2. Influence of bolt pretension force on anti-slip load of the new connection

Stress relaxation is a common phenomenon in metal material connections [27]. After the final tightening of high-strength bolts, their pretension will lose to a certain extent due to the influence of plate thickness, bolt diameter, temperature, time, etc., resulting in a reduction in the clamping force of the components. Especially for friction-type high-strength bolts, this will cause a great loss of their shear resistance. On the other hand, T-type connections are often used in steel structure connections, such as rigid joint connections of frame structures, end plate connections, etc. These connections bear a certain bending moment while bearing slip loads [28], which increases the internal force of some bolts [29-30], as shown in Fig.20. Since the tension in these connections usually does not act exactly on the bolt axis, but is transmitted through plates, angle steels or T-section steels that are in vertical contact with the bolt shank, the clamping force between them and the connecting plate is reduced, the friction force is decreased, and thus the shear resistance of the entire connection is lowered.

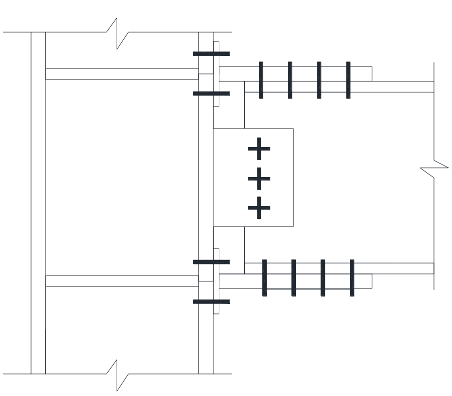
(a) Rigid joint

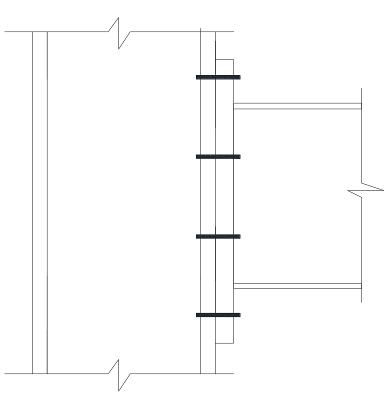
(b) Plate end connection

Fig. 20 Bolted connections subjected to tension

Therefore, the research on the influence of changes in pretension force on the anti-slip performance of the new type of anti-slip connection with particles embedded into ordinary steel is particularly important. The data on the anti-slip load of the connection under different pretension forces are analyzed and shown in Table 13.

Table 13
Anti-slip loads of connections under different pretension conditions

Pretension/kN	Particle diameter d/mm	No particle	1 particle	2 particles	4 particles
8.58	2	3.39	6.77	8.78	12.67
21.32	2	8.63	12.39	14.36	17.79

To more clearly analyze the shear resistance effect of particles in the connection, Eq.(2) is used to derive $N_{pv} = F_{sc} - N_f$. After excluding the factor of frictional resistance between the connecting plates, Table 14 is obtained.

Table 14
The anti-slipping load provided by the particles

Pretension/kN	Particle diameter d/mm	1 particle	2 particles	4 particles
8.58	2	3.38	5.39	9.28
21.32	2	3.75	5.73	9.31

A comparison of the data in Table 14 reveals that the magnitude of the bolt pretension has little impact on the anti-slip effect exerted by the particles. When a connection is subjected to tension under external forces, the pretension of high-strength bolts will be partially released, leading to a decrease in the frictional force between the connecting plates. However, for the new type of connection, the particles can still exert a strong shear resistance effect at this time, ensuring the effectiveness of the connection. This reflects that the new anti-slip connection structure with embedded particles can better ensure the stability of the connection's anti-slip load compared with high-strength bolt friction-type and high-strength bolt bearing-type connections.

4.3.3. Influence of the number of particles on the anti-slip load of the new connection

A horizontal comparison of data in Table 11 shows that, unlike the particle embedding test results, the anti-slip load provided by particles in the connection tests does not increase proportionally with the number of particles. After an in-depth analysis of the data, the structure of the new connection, and the test method, the following two main influencing factors are summarized: (1) The impact of the increase in the number of particles on the increase in the resilience of the connecting plate. After the bolt is tightened, both the steel balls and the steel plate have a certain degree of elasticity, which leads to a decrease in the connection pretension and the clamping force of the steel plate on the particles, which may result in a reduction in the shear resistance effect of the particles. Regarding the influence of pretension, the anti-slip loads provided by particles under different pretensions are compared, as shown in Table 14. When the pretension increases by 2.48 times, the anti-slip load provided by a single particle only increases slightly (10% when 1 particle is embedded in, 3% when 2 particles are embedded in, and 0.08% when 4 particles are embedded in), and the increase tends to decrease as the number of particles increases. Moreover, in horizontal comparison, after the pretension is increased, the anti-slip load provided by a single particle still decreases significantly as the number of particles increases. This indicates that pretension is not the main reason for the decrease in the anti-slip effect of particles. (2) The impact of the connection method. To effectively determine the anti-slip performance of embedded particles and reduce other influencing factors, this test adopts a typical single-shear pre-tightened bolt connection form. However, when this connection method is used in the connection anti-slip test, since the direction of the shear force is not collinear with the length direction of the connecting plate, a bending moment will be generated between the two connecting plates, which increases with the increase of the test shear force, and the warping of the plate end gradually increases. When the plate is long, the impact of this phenomenon on conventional connections is not obvious, but for the new connection in this research, when the bending moment is large enough to cause a gap between the two connecting plates, the particles no longer fit with the embedded holes of the connecting plate, and the area of the particles bearing the slip load is greatly reduced, as shown in Fig.21. With the significant reduction in the stressed area, the anti-slip effect of a single particle is obviously reduced.

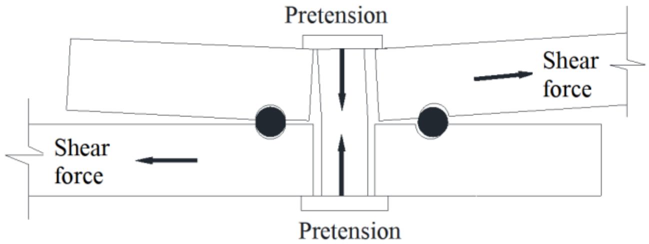

Fig. 21 The force-bearing part of the particle changes from a semicircular surface to a line

Analysis of the test phenomena reveals that when the number of particles embedded into the connecting plate is small, the depth of the plow furrows on the plate observed after the completion of the connection anti-slip test is approximately equal to the depth of the original embedded area of the particles, as shown in Fig.22. This indicates that when the particles bear the slip load, their acting surface remains relatively intact, and the gap between the connecting plates has no significant impact on the particles, allowing them to fully exert their anti-slip effect.

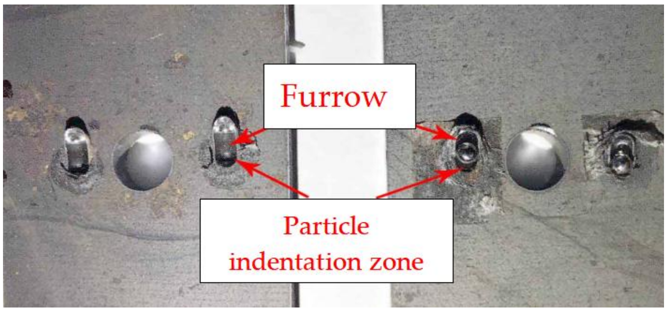

Fig. 22 Depth of furrow on the plate with little number of embedded particles

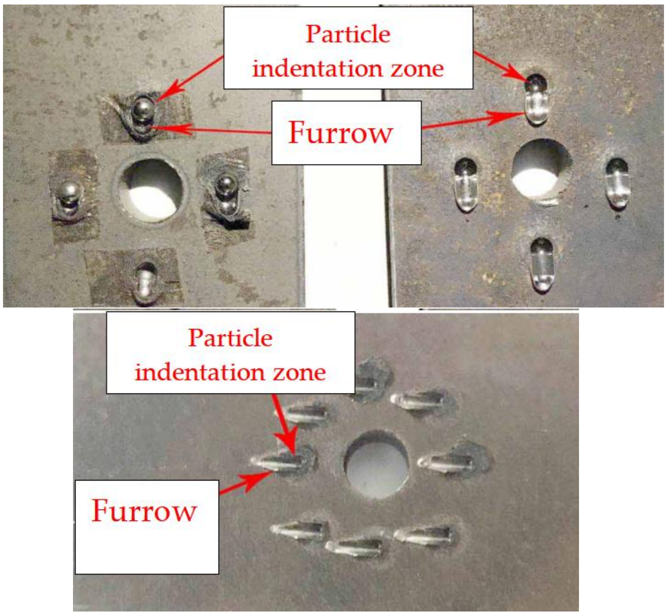

Fig. 23 Depth of furrow on the plate with large number of embedded particles

A comparison of Fig.23 shows that as the number of particles increases, after the connection is subjected to tension, the warping of the plate end gradually intensifies. At this time, the number of exposed particles and their exposed parts increase, the depth of the plow furrows gradually decreases, and the particles as well as the local plate material around the embedded holes are no longer in a state of triaxial compression. This leads to a reduction in the anti-slip effect formed by a single particle. It is suggested that in subsequent studies, a better operation method for embedding particles should be developed to facilitate the use of a double-shear connection form, thereby reducing the impact of bending moments during the process of the connection bearing slip loads. Increasing the thickness of the connecting plate and the diameter of the bolts can eliminate the influence of the warping of the connecting plate end, making the test more in line with engineering practice and preparing for the standardization of the new connection in the future. After comprehensive analysis, the adoption of the single-shear pre-tightened bolt connection form will have a certain impact on the test results, causing the effect of particles to not be fully exerted during the test. However, this does not affect the property that embedding particles into the connecting plate can improve the overall anti-slip performance of the connection. Even under the condition that the effect of the new connection is reduced, embedding 4 particles with a diameter of 3mm into the connecting plate can make its anti-slip coefficient reach 2.8, which is 5 times the anti-slip coefficient achieved by other current steel plate surface treatment methods, as shown in Table 15 [23,26]. This indicates that the new connection has extremely high value.

Table 15
Comparison of slip resistance coefficients of different surface treatment methods

Surface treatment method	Anti-slip coefficient (μ)
Grinding with a grinding wheel	0.35–0.45
Sandblasting/shot peening	0.40–0.50
Applying inorganic zinc-rich paint after sandblasting	0.45–0.55
Generating red rust after sandblasting	0.40–0.50
Proposed particle embedding (4×3mm particles)	2.80

4.3.4. Fatigue life consideration

Indentations formed by particle embedding may act as stress concentration sources, which may affect the fatigue life of the connection under cyclic loads. It was observed in the experiment (Section 3.2) that there were no cracks at the edge of the indentation, and the surface of the connecting plate was in a triaxial compressive stress state after particle embedding (Section 4.3.1), which could partially inhibit stress concentration. Referring to the GB50017-2017 specification and relevant literature, the influence of the indentation size (maximum depth ≤ 3.5mm) on the fatigue life of Q345B steel can be controlled within 10%. In engineering applications, it is recommended that particles be arranged away from welds and high stress concentration areas, and the edges of indentations be slightly ground with a grinding wheel (roughness $R_a \leq 3.2\mu m$) to further reduce fatigue risks.

The particle-embedded connection shows high slip resistance coefficient and stable load-bearing capacity. The slip resistance mechanism is mainly related to the shear deformation of particles and the plastic flow resistance of the surrounding material of the indentation. Through reasonable design and construction measures, the influence of indentations on fatigue life can be effectively controlled.

4.3.5. Durability and corrosion resistance

The coupling of dissimilar metals (GCr15 particles and Q345B steel) may cause galvanic corrosion, so it is necessary to discuss the performance in humid environments and corresponding protective measures. The potential difference between GCr15 and Q345B is small (≤ 0.1V), so the risk of galvanic corrosion is low. The tiny gaps formed after particle embedding can be sealed by applying inorganic zinc-rich paint to avoid water vapor intrusion. In marine or high-humidity environments, it is recommended to use galvanized bolts with sealants to further improve corrosion resistance.

4.3.6. Double-shear connection performance

The single-shear test adopted in this study has the problem of warpage (prying force) of the connecting plate under load. It is necessary to discuss the performance of this problem in the actual double-shear connection. In the actual double-shear connection, the connecting plates on both sides of the bolt are symmetrically stressed, so the warpage (prying force) is significantly inhibited, the fit between particles and indentations is higher. In terms of force flow characteristics, in the double-shear connection, the particles uniformly bear the shear force, and there is no local exposure phenomenon. The anti-slip load increases approximately linearly with the number of particles, which is in contrast to the nonlinear growth in the single-shear test. This linear growth characteristic is more conducive to the design and calculation of engineering applications.

5. Suggestions for anti-slip connection design

The particle-embedded slip-resistant connection proposed in this study exhibits excellent anti-slipping performance, which provides a new idea for improving the slip resistance of steel structure connections. To promote industrial application, two feasible industrial-grade application schemes are proposed: Scheme 1 (factory pre-embedding): During the production or processing of steel plates, special molds are used to position the particles, and GCr15 steel balls are pressed into the preset positions by automatic pressure equipment (the pressing parameters are controlled according to the fitting formula in Section 3.3), ensuring uniform particle embedding depth and avoiding on-site operation errors. Scheme 2 (particle-integrated gasket): A high-strength steel gasket with reserved particle grooves is designed, and GCr15 particles are pre-fixed in the gasket grooves. During on-site installation, only the conventional bolt connection process is required, and the particles are naturally embedded into the surface of the connecting plate with the bolt preload, reducing construction complexity.

Future research will focus on optimizing the design parameters of the connection, verifying the long-term service performance of the two industrial application schemes proposed above, and carrying out full-scale model tests to provide more reliable data support for engineering applications.

6. Conclusions

This paper mainly conducts experimental verification and research on the innovative concept of the new connection formed by embedding particles into ordinary steel. Particle embedding tests and anti-slip tests were carried out, and the calculation formulas were fitted. The main conclusions are as follows:

(1) With the increase in the number of particles, the embedding load basically increases proportionally. When single GCr15 bearing steel balls with diameters of 1.5mm, 2mm, 2.5mm, 3mm, and 3.5mm are embedded into the surface of the connecting steel plate respectively, the minimum embedding loads required are 4.13kN, 7.41kN, 10.95kN, 17.22kN and 22.49kN.

(2) As the diameter and quantity of embedded particles increase, the anti-slip coefficient of the connection increases significantly. After 4 particles with a diameter of 3mm are embedded into the connecting plate, the anti-slip coefficient of the connection reaches 2.8, which is 5 times that of other current treatment methods.

(3) With the increase in the number of particles, the main factor leading to the decrease in the shear resistance effect of a single particle in the particle group embedded into the steel plate is the limitation of the single-shear connection mode. That is, when the number of particles increases and the overall shear resistance of the connection increases, the warping of the connecting plate becomes more obvious, and some particles are exposed, resulting in a decrease in the shear resistance effect of a single particle.

(4) After the bolt pretension exceeds the critical value, it has little impact on the anti-slip effect of the particles. When the friction between connecting plates decreases due to the tension on the connection or the relaxation of the connection pretension, the particles can still exert their shear resistance effect. Compared to friction-type high-strength bolted connections, the new particle-embedded anti-slip connection better ensures the stability of the anti-slip load.

References

[1] J. Zhao, Y. Peng, H.X. Li, et al. Structural properties of cold-formed thin-walled rectangular high-strength stainless-steel spliced tubular columns under axial compression and compression-bending. Adv Steel Constr. 2025;24(3):182-193.

[2] H. Yin, H.S. Zhang, Q. Song, et al. Splitting of inorganic-bonded bamboo composite beams loaded perpendicular to the grain by bolted connections. Eng Struct. 2025;343:121091.

[3] V. Natesan, B. Shanmugasundaram, M. Madhavan. Comparative experimental studies on the web cleat bolted CFS beam-to-column connection. J Constr Steel Res. 2020;170:106080.

[4] M.Q. Wang, X.B. Song, X.L. Gu, et al. Bolted glulam beam-column connections under different combinations of shear and bending. Eng Struct. 2019;181(15):281-292.

[5] X.B. Song, Y.Q. Ma, X.L. Gu, et al. Carbon fiber–reinforced polymer reinforcement for rotational behavior of bolted glulam beam-to-column connections. J Compos Construct. 2017;21(3):04016096.

[6] T.Q. Xu, Y.R. Ma, X.B. Song, et al. Experimental study on rotations behavior of bolted glulam beam-to-column connections with slotted-in flanged steel plates. J Build Struct. 2017;38(9): 131-137. (in Chinese)

[7] M. Deng, X.B. Song, Y. Gao. Experimental study of rotational behavior of bolted glulam beam-to-column connections with two-part steel section. J Build Struct. 2023;44(10):97-105. (in Chinese)

[8] Y.X. Shi, K. Jiang, M.D. Wang, et al. Experimental and numerical study of full-scale column-base connections with enlarged bolt holes infilled by high strength grout. Eng Struct. 2025;341:120839.

[9] W. Zhao, S. Lu, X. Jing. Shear performance of high-strength bolt connector considering different pad and bolt hole. Struct. 2020;28:1291-1300.

[10] J. Pan, R. Huang, J. Xu, et al. Behavior of exposed column-base connections with four internal anchor bolts under seismic loading. Struct. 2021;34:105-119.

[11] S. Xiao, G.J. Sun, J.Z. Wu, et al. Study on anti-slip bearing capacity of cable clamp joints of large-span spatial structure considering zinc layer material and cable type under transient high temperature. Constr Build Mater. 2025;473:141043.

[12] H.B. Liu, G.Q. Wang, J.Y. Huang, et al. Experimental and numerical study on the anti-sliding performance of full-lock coil cable clamps. J Constr Steel Res. 2021;187:106957.

[13] Z.Q. Wang, Q.H. Han, Y. Lu, et al. Anti-slip performance of cast steel cable clamps for prestressed cables. Struct. 2022;46:353-368.

[14] Y. Ruan, B. Luo, M. Ding, et al. Theoretical and experimental study on the anti-sliding performance of casting steel cable clamps. Adv Civ Eng. 2019;1:2019.

[15] N. Zhang, B. Luo, L. Huang, et al. Research on the anti-slip performance of arc groove cable clamps. J Constr Steel Res. 2024;220:108858.

[16] Y. Wang, Y. Du, S.J. Zhu, et al. Anti-sliding performance of parallel wire strand clamps at elevated temperatures. J Constr Steel Res. 2024;212:108302.

[17] M.F. Li, K. Shen. Introduction to domestic and foreign standards for steel surface treatment. Progress in Construction Steel Structures, 2007;9(6):33-60. (in Chinese)

[18] Y. Liang, F. Wu, X.M. Huang, et al. Research and application of surface treatment technology for high-strength bolted joint surfaces of steel bridges. Science, Technology and Management (Wuhan), 2012;(1):13-17. (in Chinese)

[19] J. Ding, Y. Zou, X. Cai, et al. Study on mechanical properties of high-strength friction energy-dissipating bolts. Steel Construction, 2017;32(10):38-43. (in Chinese)

[20] Q.C. Li, Q. Gu, M.Z. Su, A.G. Chen. Experimental study on connection performance of friction-type high-strength bolts. Journal of Xi'an University of Science and Technology, 2003;23(3):322-324. (in Chinese)

[21] G. Liu, Q.C. Li, A.J. Hu. Experimental study on connection performance of high-strength bolts with sandblasted contact surface. Journal of Suzhou Institute of Science and Technology, 2009;22(3). (in Chinese)

[22] K.J.R. Rasmussen. Full-range stress-strain curves for stainless steel alloys. J Constr Steel Res. 2003;59(1):47-61.

[23] Z.X. Chen, Y. Peng, J. Dong, et al. Experimental investigation on anti-slipping performance of stainless steel slip-resistant connections with particles embedded in connected plates. Constr Build Mater. 2017;152:1059-1067.

[24] H. Aoki. Establishment of design standards and current practice for stainless steel structural design in Japan. J Constr Steel Res. 2000;54(1):191-210.

[25] Z.Q. Wang, Q.H. Han, et al. Anti-slip performance of cast steel cable clamps for prestressed cables. Struct. 2022;46:353-368.

[26] GB50017-2017. Standard for design of steel structures. China Standards Press, 2017. (in Chinese)

[27] M.Z. Song, Y. Wang, L.H. Guo. Study on pre-tension loss of high-strength bolts for steel structures. Building Technology, 2011;42(11):1033-1035. (in Chinese)

[28] Y.W. Min, W. Bao, X.Q. Zhou, et al. Analysis on code design methods for tensioned high-strength bolts in T-joints[J]. Construction Technology, 2017;1:588-591. (in Chinese)

[29] G. Shi, Y.J. Shi, Y.Q. Wang, et al. Study on mechanical behavior of high-strength bolts in end-plate connections with different configurations. Journal of Harbin Institute of Technology, 2005;37(1):66-69. (in Chinese)

[30] M.Z. Song, S.X. Zhang, Y. Wang. Experimental study on pre-tension control of friction-type high-strength bolts and anti-slip coefficient of joint surfaces. Sichuan Building Science, 2011;37(2):42-45. (in Chinese)